JOURNAL OF BACTERIOLOGY, Mar. 2001, p. 1961–1973 Vol. 183, No. 6
0021-9193/01/$04.00+0 DOI: 10.1128/JB.183.6.1961–1973.2001

Essential Thioredoxin-Dependent Peroxiredoxin System from *Helicobacter pylori*: Genetic and Kinetic Characterization

LAURA M. S. BAKER,[1] AUSRA RAUDONIKIENE,[2]† PAUL S. HOFFMAN,[2] AND LESLIE B. POOLE[1]*

Department of Biochemistry, Wake Forest University School of Medicine, Winston-Salem, North Carolina,[1] and Department of Microbiology and Immunology, Dalhousie University, Halifax, Nova Scotia B3H 4H7, Canada[2]

Received 18 October 2000/Accepted 3 January 2001

***Helicobacter pylori*, an oxygen-sensitive microaerophile, contains an alkyl hydroperoxide reductase homologue (AhpC, HP1563) that is more closely related to 2-Cys peroxiredoxins of higher organisms than to most other eubacterial AhpC proteins. Allelic replacement mutagenesis revealed *ahpC* to be essential, suggesting a critical role for AhpC in defending *H. pylori* against oxygen toxicity. Characterization of the *ahpC* promoter region divulged two putative regulatory elements and identified the transcription initiation site, which was mapped to 96 and 94 bp upstream of the initiation codon. No homologue of *ahpF*, which encodes the dedicated AhpC reductase in most eubacteria, was found in the *H. pylori* genome. Instead, homologues of *Escherichia coli* thioredoxin (Trx) reductase (TrxR, HP0825) and Trx (Trx1, HP0824) formed a reductase system for *H. pylori* AhpC. A second Trx homologue (Trx2, HP1458) was identified but was incapable of AhpC reduction, although Trx2 exhibited disulfide reductase activity with other substrates [insulin and 5,5′-dithiobis(2-nitrobenzoic acid)]. AhpC interactions with each substrate, Trx1 and hydroperoxide, were bimolecular and nonsaturable (infinite V_{max} and K_m values) but rapid enough (at 1×10^5 to 2×10^5 M^{-1} s^{-1}) to suggest an important role for AhpC in cellular peroxide metabolism. AhpC also exhibited a wide specificity for hydroperoxide substrates, which, taken together with the above results, suggests a minimal binding site for hydroperoxides composed of little more than the cysteinyl (Cys49) active site. *H. pylori* AhpC was not reduced by *Salmonella typhimurium* AhpF and was slightly more active with *E. coli* TrxR and Trx1 than was *S. typhimurium* AhpC, demonstrating the specialized catalytic properties of this peroxiredoxin.**

Infection with *Helicobacter pylori*, a microaerophilic, gram-negative bacterium, is associated with type B gastritis and peptic ulcer disease and is a risk factor for gastric carcinomas in humans (8, 17, 27). It so prevalently affects the world population that *H. pylori* has been described as "the most common chronic infection" (http://www.cdc.gov/ncidod/dbmd/diseaseinfo/hpylori_t.html), with some developing countries experiencing nearly 100% infection rates. While *H. pylori* infection is generally controlled with a cocktail of antibiotics and bismuth (60), the specter of emerging antibiotic resistance necessitates the search for alternative drug strategies and a clearer understanding of bacterial defense systems.

H. pylori colonizes the mucosal layer of the stomach and secretes immunogenic products that recruit macrophages and polymorphonuclear leukocytes to the site of infection (59). Here, the resulting oxidative burst by the phagocytic cells produces reactive oxygen species (ROS), such as superoxide anion ($O_2^{\cdot -}$), hydrogen peroxide (H_2O_2), and the hydroxyl radical ($OH^{\cdot -}$), that damage gastric tissues. Increased ROS levels are present in *H. pylori* patients (19), and it is thought that long-term exposure to ROS contributes to the development of cancerous gastric cells (16).

To resist oxidative damage from chronic inflammation, *H. pylori* relies on a variety of protective enzymatic systems, including catalase (the *katA* gene product) (47) and superoxide dismutase (the *sodB* gene product) (63), which eliminate H_2O_2 and $O_2^{\cdot -}$, respectively; however, it is unknown how *H. pylori* coordinates its oxidative stress response because the bacterium lacks the oxidatively activated regulatory genes, *soxRS* and *oxyR*, common to other eubacteria (67). We report herein that *H. pylori* also expresses a thioredoxin (Trx)-dependent alkyl hydroperoxide reductase (AhpC) protein, a member of the peroxiredoxin (Prx) family (62), whose activity can detoxify lipid hydroperoxides analogous to those created in membranes exposed to ROS (32). All Prx enzymes are dimers, decamers, or, in some cases, higher-order aggregates (1, 38, 61) with one essential, N-terminal Cys residue per subunit (Cys46 of *Salmonella typhimurium* AhpC) (21). Some Prxs contain only this single, conserved Cys (the 1-Cys Prxs), but most include another conserved Cys residue (the 2-Cys Prxs) analogous to Cys165 in *S. typhimurium* AhpC, which links the two subunits via an intersubunit disulfide bond with the N-terminal Cys in the oxidized protein (21, 53). Reduced *S. typhimurium* AhpC directly converts hydroperoxides to alcohols with concomitant formation of a sulfenic acid (Cys-SOH) at Cys46; condensation between the two active-site cysteinyl derivatives then regenerates the stable intersubunit disulfide bond of the oxidized protein (20, 21).

Our search of the *H. pylori* genomic database for an AhpC homologue revealed a gene (*ahpC*, HP1563) that had previously been reported to encode a species-specific antigen by O'Toole et al. (48). Although not identified as a peroxidase at that time, the *H. pylori* AhpC sequence containing the two conserved Cys residues was later classified as a 2-Cys Prx (12).

* Corresponding author. Mailing address: Wake Forest University School of Medicine, Department of Biochemistry, Medical Center Blvd., Winston-Salem, NC 27157. Phone: (336) 716-6711. Fax: (336) 716-7671. E-mail: lbpoole@wfubmc.edu.

† Present address: Aventis Pasteur Ltd., Toronto, Ontario M2R 3T4, Canada.

TABLE 1. Primers used to amplify and subclone *H. pylori* structural genes

Expression vector and gene	Primer (5′–3′)	
	Forward	Reverse
pPROK1		
ahpC	CGCCCGGGAGGAGGAAGAATAGATGTTAGTTACAAAACTTGCC	CCCTGCAGCTACAGCTTGATGGAATTTTCTTTAAGAT
trx1	CGCCCGGGAGGAGGAAGAATAGATGAGTCACTATATTG	CCCTGCAGTTAGCCTAAAAGTTTGTTCAATTGC
trx2	GCGAATTCAGGAGGAAGAATAGATGTCAGAAATGATTAACGGG	GCAAGCTTCCCCTTACAATAACGCTTTTAGAGC
trxR	CGCCCGGGAGGAGGAAGAATAGATGATAGATTGCGCGATTATTGG	CCAAGCTTGATTTAATGGTG
pBluescript-SK		
ahpC	TGGAATTCGCCCAATAACGATGAAACAAG	GAGAGCTCCGATTAAAGCTTAATGGA

To reduce AhpC, most bacteria, including *S. typhimurium*, express a specialized flavoprotein reductase, AhpF, which is homologous to *Escherichia coli* Trx reductase (TrxR), except that AhpF contains an additional N-terminal region directly involved in AhpC reduction (54, 55). Alternatively, some eukaryotic Prx systems utilize TrxR and Trx to reduce the peroxidase (sometimes referred to as Trx-dependent Prxs or TPxs), where TrxR catalyzes the reduction of Trx, which, in turn, reduces the Prx disulfide bond. In these cases, electron transfer proceeds along the following path: NADPH → TrxR → Trx → AhpC (TPx) → ROOH.

While eukaryotic examples of Trx-dependent Prx proteins abound (e.g., *Entamoeba histolytica* AhpC [52], *Saccharomyces cerevisiae* TPx [10], and multiple human Prx homologues [11]), to our knowledge, only one other bacterial Trx-dependent Prx, besides the *H. pylori* AhpC described herein, has been experimentally demonstrated [TPx from the cyanobacterium *Synechocystis* (75)]. A distantly related Prx family member, *E. coli* bacterioferritin comigratory protein, has also been shown to exhibit low levels of Trx-dependent peroxidase activity (34). Inspection of the *H. pylori* genome yielded no *ahpF*, but an *E. coli trxA* homologue (*trx1*, HP0824 in the annotation of Tomb et al. [67]) encoding Trx1 was identified along with an *E. coli trxB* homologue (*trxR*, HP0825) encoding TrxR. Further examination uncovered HP1164, annotated as a TrxR locus due to its similarity to *Plasmodium falciparum trxR* (21% identity). HP1164 does not, however, encode a putative catalytic disulfide motif (CXXC or CXXXXC) indicative of such a redox center and was therefore excluded from these studies. Further genomic searches revealed a second Trx locus (*trx2*, HP1458) encoding Trx2. Therefore, we considered TrxR (HP0825)-Trx1 (HP0824) and TrxR (HP0825)-Trx2 (HP1458) to be good candidates as AhpC-reducing systems.

Herein, we present the first example of a Trx-dependent alkyl hydroperoxide reductase system from a gastric pathogen and describe the cloning, purification, and kinetic characterization of AhpC, Trx1, Trx2, and TrxR from *H. pylori*. Along with the genetic characterization of *H. pylori ahpC*, we have also shown that AhpC plays a critical role in the defense against oxygen toxicity that is essential for survival and growth, even in microaerophilic environments.

(Abstracts reporting some of this information have been published earlier [5, 6]).

MATERIALS AND METHODS

Materials. Sodium dodecyl sulfate (SDS), ultrapure glycine, ultrapure urea, EDTA, dithiothreitol, Tris base, and other buffer reagents were purchased from Research Organics (Cleveland, Ohio). Bacteriological medium components were from Difco Laboratories (Detroit, Mich.). Ethanol was obtained from Warner Graham Company (Cockeysville, Md.). Isopropyl-β-D-thiogalactopyranoside (IPTG) and 5-bromo-4-chloro-3-indolyl-β-D-galactopyranoside (X-Gal) stocks were from Inalc (Milan, Italy). Vent DNA polymerase, Moloney murine leukemia virus reverse transcriptase, and T4 polynucleotide kinase were purchased from New England Biolabs (Beverly, Mass.). Restriction enzymes, ligase, calf intestinal phosphatase, and restriction buffers were obtained from Promega (Madison, Wis.). Agarose medium EEO (electrophoresis grade) and H_2O_2 were from Fisher (Fairlawn, N.J.). Acrylamide-Bis (40%) solution was purchased from Bio-Rad (Hercules, Calif.). Ampicillin (AMP) powder, cumene hydroperoxide (CHP), glucose-6-phosphate, glucose-6-phosphate dehydrogenase, linoleic acid, lipoxygenase, and insulin were from Sigma (St. Louis, Mo.). Ethyl hydroperoxide (EtOOH) was from Polysciences, Inc. (Warrington, Pa.), and *tert*-butyl hydroperoxide (*t*-BOOH) was from Aldrich (Milwaukee, Wis.). NADPH and NADH were from Roche Molecular Biochemicals (Mannheim, Germany).

RNA isolation and primer extension analysis. For RNA isolation, 50 ml of *H. pylori* strain HP 26695 (67) was grown in *Brucella* broth supplemented with 10% fetal calf serum (Sigma) in a microaerobic environment (7% O_2, 5% CO_2) at 37°C to an optical density at 590 nm of 1.0 and harvested by centrifugation at 4°C for 10 min. Cells were lysed in 50 mM Tris-HCl (pH 8.0)–1 mM EDTA–50 mM NaCl buffer supplemented with 1.5% SDS for 5 min at 95°C. Following phenol extraction and precipitation, the RNA was dissolved in diethylpyrocarbonate-treated water and the total RNA concentration was determined at 260 nm. For the primer extension studies, an oligonucleotide (5′-GCCAGAAGAA AAGAATCGCACCGT-3′; Gibco-BRL Custom Primers) was 5′- end labeled in the presence of [γ-^{32}P]ATP (5,000 Ci/mmol; Amersham) and 20 U of T4 polynucleotide kinase. Total *H. pylori* RNA (100 μg) was incubated with the ^{32}P-labeled oligonucleotide and annealed under the following conditions: 80°C for 5 min, 65°C for 5 min, 42°C for 10 min, and 37°C for 20 min. Following annealing, the RNA was precipitated with ethanol, dried, and resuspended in 7 μl of diethylpyrocarbonate-treated water and 13 μl of reverse transcriptase buffer (50 mM Tris-HCl at pH 8.3, 30 mM KCl, 10 mM $MgCl_2$, 1 μg of actinomycin D [Sigma], 1 mM dithiothreitol, 2.5 mM each deoxynucleoside triphosphate). One microliter of Moloney murine leukemia virus reverse transcriptase (50 U/μl) was added to the sample, and reverse transcription was carried out at 42°C for 60 min; 1 μl of 0.5 M EDTA and 1 μl of RNase (10 mg/ml) were added, and the reaction mixture was incubated at 37°C for an additional 30 min. The reaction was stopped by phenol-chloroform extraction, followed by ethanol precipitation. The sample was then dried and resuspended in 10 μl of sequencing loading buffer. In parallel, dideoxy DNA sequencing of the cloned *ahpC* gene and the upstream region was performed using the same oligonucleotide primer to determine the transcriptional start site. After denaturation at 95°C for 2 min, aliquots were subjected to 6% urea polyacrylamide gel electrophoresis (PAGE) and autoradiographed.

Allelic replacement mutagenesis of *ahpC*. Genomic DNA isolated from *H. pylori* strain 26695 (67) was used to amplify *ahpC* with forward and reverse oligonucleotide primers (Table 1) under typical PCR conditions to generate a product 930 bp long. Isolated *ahpC* was digested at flanking *Eco*RI and *Sac*I sites and then inserted into pBluescript-SK (+) plasmid vector (Stratagene, La Jolla, Calif.) digested with the same restriction enzymes. Vector derivatives of pBluescript were stably maintained in *E. coli* strains but were not replicated in *H. pylori* hosts. The *ahpC*-containing plasmid was then digested with *Xba*I (located approximately 330 bp from the *ahpC* translational start site), and a chloramphenicol resistance (*camR*) cassette originating from *Campylobacter coli* (70) digested with *Xba*I was inserted to interrupt the coding sequence of *ahpC*. Four *H. pylori* strains were transformed with the *ahpC*::*camR* construct: 26695 (67), SS1 (40), HP1 (28), and HP1061 (25). The same strains were also transformed with a construct in which the nitroreductase gene (*rdxA*) was interrupted with *camR*

(26). *H. pylori* transformation (electroporation) and subsequent evaluation of any colonies obtained after up to 7 days of incubation in selective medium were carried out as described elsewhere (57).

Cloning of *ahpC, trx1, trx2*, and *trxR* into expression vectors. The *H. pylori* genomic database was searched for genes corresponding to the *E. coli* sequences for *ahpC, trxA, trxB*, and *trxC* (www.tigr.org/tdb/mdb/hpdb/hpdb.html). Clones GHPDQ26, GHPAB86, GHPCL04, and GHPAE26, containing *trx1, trx2, trxR*, and *ahpC*, respectively, were ordered from The Institute of Genomic Research-ATCC Microbial Genome Special Collection. Plasmid DNA was purified from the *E. coli* host using the Wizard Miniprep Kit (Promega). The genes of interest were amplified using PCR primers (listed in Table 1) synthesized in the DNA Synthesis Core Laboratory of the Comprehensive Cancer Center of Wake Forest University. PCR mixtures (50 μl) contained 300 μM deoxynucleoside triphosphates, 1 U of vent polymerase, 10 pmol each of the forward and reverse oligonucleotides, 0.5 mM $MgCl_2$, and 0.5 μg of template DNA. Reactions were carried out as follows in a Mini Cycler (MJ Research, Waltham, Mass.): 95°C for 30 s, 40°C for 45 s, and 72°C for 1.5 min (5 cycles); 98°C for 30 s and 72°C for 1 min (35 cycles); and then 72°C for 15 min. The PCR products were purified using the QIAquick PCR Cleanup kit (Qiagen, Studio City, Calif.). The PCR products, 600 bp for *ahpC*, 300 bp for *trx1* and *trx2*, and 932 bp for *trxR*, were each separately ligated into the pCR2.1 TA cloning vector (Invitrogen, Carlsbad, Calif.). Plasmids containing each insert were digested with the restriction enzymes corresponding to the engineered restriction sites (Table 1), and then DNA fragments of interest were excised from agarose gels and purified using the Gene Clean II Kit (Bio 101, Inc., Vista, Calif.). These fragments were inserted, using T4 DNA ligase, into pPROK1 expression vectors (Clontech, Palo Alto, Calif.; expression under control of the *tac* promoter), appropriately digested, isolated from agarose gels, and pretreated with calf intestinal phosphatase.

Bacterial strains and culture procedures. Ligated DNA was transformed into competent *E. coli* XL-1 Blue cells (Stratagene), except the AhpC-expressing plasmid, which was transformed into an *ahpCF* deletion strain of *E. coli*, TA4315 (65). Single colonies were selected on Luria-Bertani (LB) plates containing AMP at 50 μg/ml, and those containing the recombinant DNA were evaluated for protein expression on SDS-polyacrylamide gels after induction with 0.4 mM IPTG. Isolated plasmid DNA for each construct was sequenced throughout the coding region by automated DNA sequencing at the Comprehensive Cancer Center of Wake Forest University. Bacterial stocks containing each plasmid with the subcloned gene were prepared from a single colony and stored at −80°C in LB broth containing 15% (vol/vol) glycerol. Culture procedures were generally the same as reported earlier (53).

Purification of recombinant AhpC. Purification of AhpC was performed as described earlier (53), with some modifications. All procedures were carried out in a standard buffer (pH 7.0) consisting of 25 mM potassium phosphate with 1.0 mM EDTA. Briefly, 100 ml of *E. coli* TA4315 harboring the pPROK1/*ahpC* plasmid was added to 10 liters of LB medium containing 0.5 g of AMP supplemented with 0.2% glucose in a BioFlo 2000 fermentor (New Brunswick Scientific, Edison, N.J.). IPTG (0.4 mM) was added at $A_{600} = 0.9$, and bacteria were harvested by centrifugation 16 h after induction. Pelleted bacteria were disrupted with a Bead Beater (BioSpec Products, Bartlesville, Okla.), cell extracts were treated with streptomycin sulfate to precipitate nucleic acids, and 20 and 60% ammonium sulfate treatments were carried out to precipitate proteins as described previously (53). The protein resuspended in standard buffer containing 20% ammonium sulfate was applied to a Phenyl Sepharose 6 Fast Flow Column (24 by 2.5 cm; Pharmacia LKB Biotechnology Inc.), washed with 20% ammonium sulfate buffer, and eluted with a linear gradient of 20 to 0% ammonium sulfate in standard buffer. Protein fractions were evaluated for purity of overexpressed AhpC by SDS-PAGE, and the purest fractions were pooled. After dialysis against 10 mM potassium phosphate buffer (pH 7.0), the protein was loaded onto a DEAE-cellulose column (24 by 2.5 cm; Whatman DE52) and eluted with a linear gradient of 10 to 100 mM potassium phosphate (1-liter total volume). Again, fractions were analyzed for AhpC by SDS-PAGE and pure fractions were pooled, concentrated, and aliquotted for storage at −20°C.

Purification of recombinant Trx1. A 10-liter culture of *E. coli* XL-1 Blue harboring the pPROK1/*trx1* plasmid was grown in the fermentor and induced as described above for AhpC expression. The crude cell extract obtained as described above was treated with streptomycin sulfate, and following centrifugation, the supernatant was subjected to heat denaturation at 70°C for 4 min to remove contaminating proteins. Denatured proteins were removed via centrifugation at 23,000 × *g* for 20 min, and the supernatant was dialyzed overnight in three changes (6 liters each) of 5 mM potassium phosphate buffer (pH 7.0). The dialyzed protein was applied to a DEAE-cellulose column (24 by 2.5 cm; Whatman DE52) pre-equilibrated with 10 mM potassium phosphate (pH 7.0). Trx1 eluted upon application of a linear gradient of 10 to 100 mM potassium phosphate (1-liter total volume) and was identified by SDS-PAGE. Pooled fractions were concentrated to 2 ml, and the concentrate was applied to a BioGel A-0.5 m agarose column (Bio-Rad) equilibrated in the standard buffer. The fractions were collected, assessed for purity using SDS-PAGE, pooled, and aliquotted for storage at −20°C. Further molecular weight and purity analysis required the use of Tris-Tricine gels as described by Ausubel et al. (3).

Purification of recombinant TrxR. A 10-liter culture of XL-1 transformed with the pPROK1/*trxR* plasmid was grown, induced, and harvested; the crude extract was prepared essentially as described for AhpC. After the 60% ammonium sulfate treatment, the resuspended and dialyzed protein was loaded onto the DEAE-cellulose column and eluted as described for Trx1. Purified fractions, as assessed by the ratio of A_{280} to A_{450}, were pooled and loaded onto an Affi-Gel Blue column (24 by 2.5 cm; Bio-Rad). Fractions were eluted with a linear gradient of 25 mM potassium phosphate buffer to 600 mM potassium phosphate and 0.3 M NaCl (pH 7.0; 700-ml total volume). Protein purity was assessed by A_{280}/A_{450} ratio determination and SDS-PAGE. Pure fractions were pooled, dialyzed in standard buffer, and aliquotted for storage at −20°C.

Purification of recombinant Trx2. A 10-liter culture of XL-1 transformed with the pPROK1/*trx2* plasmid was grown under the conditions described for Trx1. Bacteria containing Trx2 were treated as described for Trx1, except for the following modifications. Instead of heat denaturation, the supernatant from an initial treatment with 50% ammonium sulfate was brought to 80%. The pelleted protein was resuspended in 5 mM potassium phosphate buffer, dialyzed overnight in the same buffer, and applied to the DEAE-cellulose column pre-equilibrated with 5 mM potassium phosphate buffer (pH 7.0). The nonbinding fraction was then applied to a carboxymethyl cellulose column (24 by 2.5 cm; Whatman CM) pre-equilibrated with 5 mM potassium phosphate buffer (pH 7.0); this was followed by elution with a linear gradient of 5 to 60 mM potassium phosphate (700-ml total volume). SDS-PAGE was again used to assess purity, and concentrated protein was aliquotted for storage at −20°C in standard buffer.

Other protein purifications. Purification of *E. coli* TrxR and Trx1 was done essentially as described by Poole et al. (54). *S. typhimurium* AhpF and AhpC were purified as reported previously (53).

Sequence analysis. AhpC homologues were identified through BLAST (2) searches with the *H. pylori* AhpC sequence. Pairwise comparisons of the *H. pylori* AhpC sequence were generated with AhpC sequences from other organisms using the BLAST Two Sequences program at the National Center for Biotechnology Information website (http://www.ncbi.nlm.nih.gov/).

Spectroscopic experiments. Most spectral assays were carried out using a thermostatted Gilford 220 updated recording spectrophotometer with a Beckman DU monochromator and a Kipp and Zonen (Delft, The Netherlands) chart recorder. Extinction coefficient determination using microbiuret assays for proteins at 280 nm and for bound flavin at 450 nm, thiol content determination using 5,5′-dithiobis(2-nitrobenzoic acid) (DTNB), and disulfide detection using 2-nitro-5-thiosulfobenzoate (NTSB) were all performed as described previously (51, 53). Further quantification of *H. pylori* proteins relied on the following extinction coefficients experimentally obtained at 280 nm (except where noted): AhpC, 24,800 ± 300 M^{-1} cm^{-1}; Trx1, 17,200 ± 1,000 M^{-1} cm^{-1}; Trx2, 23,300 ± 300 M^{-1} cm^{-1}; TrxR, 11,900 ± 110 M^{-1} cm^{-1} (450 nm). To quantitate the concentration of other proteins and reagents by absorbance, the following extinction coefficients were used: *E. coli* TrxR, 11,300 M^{-1} cm^{-1} (454 nm) (73); *E. coli* Trx1, 13,700 M^{-1} cm^{-1} (280 nm) (31); *S. typhimurium* AhpF, 13,100 M^{-1} cm^{-1} (450 nm); AhpC, 24,300 M^{-1} cm^{-1} (280 nm) (53); TNB^{2-}, 14,150 M^{-1} cm^{-1} (412 nm) (58); NADPH, 6,200 $M^{-1}cm^{-1}$ (340 nm); NADH, 6,220 M^{-1} cm^{-1} (340 nm).

Determination of H_2O_2 content using ferrithiocyanate. To monitor the disappearance of hydrogen peroxide in solution, experiments were conducted essentially as described by Thurman et al. (66), except that peroxidase reactions (0.5 ml of AhpC [20 μM], Trx1 [2.0 μM], and TrxR [0.2 μM]) were initiated with the addition of H_2O_2 (1 mM). Reactions mixtures were incubated at 37°C, and aliquots were removed at various time points up to 30 min. Reactions were terminated by the addition of 0.5 ml of 12.5% trichloroacetic acid, precipitated proteins were removed by centrifugation, and peroxide content was analyzed by ferrithiocyanate complex formation [0.2 ml of 10 mM $Fe(NH_4)_2(SO_4)_2$ and 0.1 ml of 2.5 mM KSCN were added to a 50-μl aliquot of supernatant]. Red ferrithiocyanate complex was measured at 480 nm, and peroxide concentration was determined from a standard curve with H_2O_2.

AhpC activity assays and reductase system determination. All AhpC activity assays were conducted on an Applied Photophysics DX.17 MV stopped-flow spectrophotometer at 25°C, except where noted otherwise. Aerobic, steady-state AhpC activity assays were monitored by following the decrease in A_{340} due to NADPH oxidation. All peroxidase assays were conducted with 50 mM potassium phosphate buffer (pH 7.0)–0.1 M ammonium sulfate–0.5 mM EDTA. Proteins in

one syringe were mixed with substrates in the other syringe, except where indicated otherwise. The rate of change in A_{340} was assessed by linear regression analysis of the first 10% of the linear region of the resulting trace. Preparation of the reaction chamber for anaerobic assays was conducted essentially as described previously (44).

Steady-state kinetic analysis of TrxR with Trx1. K_m and k_{cat} measurements of TrxR for NADPH and Trx1 were conducted essentially as previously described (41), except that they were carried out on the stopped-flow spectrophotometer. Assays contained 0 to 40 μM NADPH (0.2 μM at the lowest concentration), 0 to 100 μM Trx1, and 34 nM TrxR (final concentrations are indicated), and activity was followed by monitoring the change in NADPH fluorescence over time (excitation at 340 nm and emission recorded at 90° using a 400-nm filter). The decrease in fluorescence over time was converted to absorbance units per minute using a standard curve. Primary rate data were fitted to a rectangular hyperbolic function obtained using the Marquardt-Levenberg curve-fitting algorithm in SigmaPlot (Jandel Scientific, San Rafael, Calif.). The rate data obtained after varying each substrate were transformed and displayed in a primary Hanes-Wolf plot and yielded lines that intersected on the *y* axis, indicating a substituted mechanism for TrxR. A substituted (ping-pong) mechanism was then assumed for all equations, and the initial rate in the absence of products was represented by the following equation (15): $v = Vab/(K_{mB}a + K_{mA}b + ab)$, where a is the concentration of Trx1, b is the concentration of NADPH, V is the maximum velocity, and K_m is the Michaelis constant. Slopes and *y* intercepts obtained from the linear regression lines for each concentration of Trx1 were replotted in a secondary Hanes-Wolf plot to obtain the true V_{max} and K_m for each substrate. The *y* intercept of the secondary plot was equivalent to K_{mB}/V, and the slope was equal to $1/V$. To solve for K_{mA}, the following relationship was used: $V(\text{app})/K_m(\text{app}) = V/K_{mA}$, where the $V(\text{app})/K_m(\text{app})$ ratio was obtained from Michaelis-Menten plots of the initial-rate data.

The apparent K_m and V_{max} of TrxR for Trx1 and Trx2 were also determined on a thermostatted Milton Roy Spectronic 3000 diode array spectrophotometer at 340 nm using an insulin reduction assay as described by Holmgren and Bjornstedt (30). Reactions (500 μl) were conducted at 25°C in 100 mM potassium phosphate buffer (pH 7.5) with EDTA (1.5 mM) containing Trx1 or Trx2 (0 to 50 μM), insulin (80 μM), NADPH (150 μM), and TrxR (7.0 nM; added last). Kinetic parameters were obtained using the curve-fitting function in Sigma Plot as described above. Assays using DTNB (200 μM) instead of insulin were conducted essentially as described above, except that the reaction was monitored at 412 nm to observe the rate of formation of TNB^{2-}.

The oxidase activity of TrxR was measured as described earlier (53). Briefly, *H. pylori* TrxR (30 to 240 nM), *S. typhimurium* AhpF (15 to 60 nM), or *E. coli* TrxR (30 to 120 nM) was added to 500 μl of air-saturated standard buffer containing NADPH (150 μM) and the change in A_{340} was monitored. The TrxR activity of *H. pylori* TrxR or Trx1 mixed with *E. coli* TrxR or Trx1 in heterologous mixtures was determined on the Gilford spectrophotometer using the DTNB reduction assay described above. Reaction mixtures contained 0.5 to 100 μM Trx1 (from either *H. pylori* or *E. coli*) and were started with the addition of 0.5 μM TrxR (from either *H. pylori* or *E. coli*).

Bisubstrate steady-state kinetic analysis of AhpC. Aerobic peroxidase assays monitoring the A_{340} change of NADPH were carried out on a stopped-flow spectrophotometer as described above. In one syringe, peroxide substrates (10 to 40 μM) were incubated in the peroxidase assay buffer. (All concentrations shown are final concentrations achieved upon mixing.) In the other syringe, AhpC (0 to 2 μM), Trx1 (20 μM), and *E. coli* TrxR (2 μM) were incubated with NADPH (150 μM) for 5 min prior to assay with the peroxide substrate. (Use of *E. coli* TrxR rather than *H. pylori* TrxR in this assay did not significantly affect the results but did greatly decrease the problem of AhpC-independent NADPH oxidation.) The kinetic coefficients were obtained as described by Forstrom et al. (24). Data were analyzed using the integrated Dalziel rate equation for a two-substrate enzymatic system in which enzyme-substrate complexes were not experimentally observed: $E_0(t/[\text{ROH}]_t) = \phi_1 \ln([\text{ROOH}]_t/([\text{ROOH}]_0 - [\text{ROH}]_t)/[\text{ROH}]_t) + \phi_2/[\text{Trx1}] + \phi_0$, where $[\text{ROOH}]_0$ is the initial hydroperoxide concentration, $[\text{ROH}]_t$ is the product (alkyl alcohol) concentration at time t, and ϕ_1, ϕ_2, and ϕ_0 are the Dalziel coefficients. Data were chosen and analyzed as described previously for tryparedoxin peroxidase from *Crithidia fasciculata* (46). Linoleic acid hydroperoxide (LOOH) was prepared by enzymatic oxidation with soybean lipoxygenase as described by Maiorino et al. (43).

RESULTS

Amino acid sequence alignments. In an amino acid sequence comparison of the putative AhpC from *H. pylori* with the more extensively studied *S. typhimurium* enzyme, Cys49 in *H. pylori* AhpC aligns perfectly with the essential, conserved Cys46 from *S. typhimurium* AhpC (21). Cys49 in *H. pylori* AhpC is, therefore, most likely the site of interaction with peroxides and the site of sulfenic acid formation. The *H. pylori* AhpC amino acid sequence was also compared to the deduced amino acid sequences for other 1- and 2-Cys AhpC homologues from a wide range of organisms (Table 2). Of all the known homologues, *H. pylori* AhpC shares the most sequence identity with a select group of bacterial Prxs including AhpC from *Campylobacter jejuni* (67%), TPx from *Rickettsia prowazekii* (54%), and AhpC from *Legionella pneumophila* (52%). Other than the proteins from these three bacterial sources, however, *H. pylori* AhpC is more similar to 2-Cys Prx protein sequences from higher organisms than to other bacterial AhpC proteins (Table 2). Of the sequences shown, *S. cerevisiae* Prx (2-Cys), *C. elegans* Prx, the human proliferation-associated gene (2-Cys), and *Synechocystis* sp. strain PCC6803 (a cyanobacterium) TPx have all been shown experimentally to be recycled by a Trx-reducing system (10, 36, 52).

TrxR and Trx1 from *H. pylori* share a moderate amount of sequence identity (37 and 51%, respectively) with the corresponding *E. coli* homologues and a high percentage of identity (60 and 68%, respectively) with the homologues from the closely related species *C. jejuni*. As in *H. pylori*, the absence of *ahpF* in *C. jejuni* makes TrxR and Trx1 reasonable candidates as *C. jejuni*'s AhpC reductase system. *H. pylori* Trx2 shares the highest sequence identity with a Trx homologue from *Archaeoglobus fulgidus* (Trx4, 42%) (39) and is more closely related to *E. coli* Trx2 (41% identity) (45) than to *E. coli* Trx1 (33% identity) (29). Known redox centers and binding motifs of other Trx and TrxR proteins are completely conserved in the *H. pylori* proteins. Unlike the vast majority of TrxR-Trx1 systems from other bacteria, the gene encoding TrxR is positioned just downstream from *trx1* in the *H. pylori* genome. The clustering of *trx1* and *trxR* in this order has also been observed in *Streptomyces clavuligerus* (14); however, in mycobacteria (72) and in *C. jejuni* (49), the opposite orientation, *trxR* and then *trx1*, is observed. In most other species, *trxR* and *trx1* are widely separated on the chromosome. Interestingly, *H. pylori trx2* (HP1458) is not found near *trx1* (HP0824) or *trxR* (HP0825).

Characterization of purified *H. pylori* proteins. AhpC, Trx1, Trx2, and TrxR expressed from pPROK1 in the respective *E. coli* strains were purified to homogeneity (Fig. 1). All proteins were obtained in high yields as soluble proteins after induction with IPTG at 37°C. Migration of the *H. pylori* proteins was compared to that of pure *S. typhimurium* or *E. coli* homologues during SDS-PAGE, which allowed the detection of each protein during purification and assessment of purity. Pure, reduced AhpC corresponded to an apparent molecular mass of 26 kDa, which is slightly higher than its expected molecular mass of 22,235 Da. When prepared in nonreducing sample buffer and analyzed by SDS-PAGE, AhpC migrated as a 50-kDa protein, indicating that the purified protein is oxidized and contains one or more intersubunit disulfide bonds (Fig. 1A, lane 6). TrxR migrated as a 33-kDa protein on SDS-PAGE under both reducing and nonreducing conditions (Fig. 1A, lanes 5 and 7; expected mass, 33,538 Da). Previously, an intersubunit disulfide bond between TrxR subunits was suggested by Windle et al. (74); our results, however, rule out such

TABLE 2. Pairwise sequence alignments (percent identities) of *H. pylori* AhpC with AhpC homologues from other organisms

Organism[a]	Eubacteria						Archaeon, *M. jannaschii* (anaerobic)	Eukaryota (aerobic)				
		Aerobic		Anaerobic				Yeast			Human	
	H. pylori (microaerophilic)	*M. tuberculosis*	*Synechocystis*	*C. pasteurianum*	*S. mutans*	*S. typhimurium*		1-Cys *S. cerevisiae*	2-Cys *S. cerevisiae*	*C. elegans*	1-Cys *H. sapiens*	2-Cys *H. sapiens*
H. pylori	100	41	46	39	34	32	32	30	46	47	27	45
M. tuberculosis		100	37	38	32	33	26	32	36	35	32	39
Synechocystis			100	51	36	35	34	29	47	55	26	57
C. pasteurianum				100	32	34	38	32	50	53	30	52
S. mutans					100	62	27	23	34	37	22	36
S. typhimurium						100	33	30	31	37	27	37
M. jannaschii							100	45	33	36	41	40
1-Cys *S. cerevisiae*								100	29	31	48	34
2-Cys *S. cerevisiae*									100	66	28	60
C. elegans										100	29	74
1-Cys *H. sapiens*											100	31
2-Cys *H. sapiens*												100

[a] The accession numbers (National Center for Biotechnology Information database) of the sequences are as follows: AhpC of *H. pylori*, P21762; open reading frame C of *Clostridium pasteurianum*, P23161; AhpC of *Streptococcus mutans*, BAA25695; AhpC of *Salmonella typhimurium*, P19479; AhpC of *Mycobacterium tuberculosis*, CAB03768; SLL0755 of *Syechocystis* sp. strain PCC6803, Q55624; AhpC of *Methanococcus jannaschii*, AAB98731; Prx1 of *Saccharomyces cerevisiae*, CAA80784; TSA-I (type Iα TPx) of *S. cerevisiae*, P34760; AhpC/TSA of *Caenorhabditis elegans*, AAA79342; Prx (hORF6) of *Homo sapiens*, BAA03496; proliferation-associated protein TPx2 of *H. sapiens*, Q06830.

a linkage between subunits. Spectral analyses (data not shown) of TrxR revealed a strong A_{454}, which is typical of enzymes containing a bound flavin cofactor. Trx1 and Trx2 both migrated as monomers in the presence or absence of β-mercaptoethanol and gave masses of approximately 12 kDa, close to their expected masses of 11,854 and 11,744 Da, respectively.

Kinetic characterization of Trx1, Trx2, and TrxR. *H. pylori* TrxR and Trx1 were shown in a series of assays to act as a general disulfide reductase system analogous to their counterparts from *E. coli*. When assayed with small-molecule (DTNB) or protein (insulin) disulfide-containing substrates, both Trx1 and Trx2 from *H. pylori* exhibited TrxR-dependent reductase activities that were hyperbolically dependent on the Trx1 and Trx2 concentrations. Insulin reduction in vitro by TrxR-Trx1 gave a V_{max}(app) of 19.9 ± 1.4 μM min^{-1} and a K_m(app) for Trx1 of 13.4 ± 2.7 μM (Fig. 2), while the TrxR-Trx2 system gave a V_{max}(app) of 10.6 ± 1.5 μM min^{-1} and a K_m(app) for Trx2 of 11.0 ± 1.9 mM (Fig. 2). While Trx2 exhibited about half of the turnover rate of Trx1 in insulin assays, both Trx1 and Trx2 reduced the small, non-protein disulfide substrate DTNB with about the same catalytic parameters as the TrxR-Trx1-insulin system (Fig. 2). In TrxR-Trx1-insulin experiments in which NADPH was replaced with NADH, no decrease in the NADH A_{340} was observed upon addition of TrxR to the reaction mixture, demonstrating the high specificity of TrxR for NADPH. *H. pylori* TrxR and Trx1 were also capable of forming an efficient reducing system when mixed with their *E. coli* counterparts (data not shown). Using the DTNB-linked TrxR assay, reaction mixtures containing one *H. pylori* reductase component mixed with a corresponding *E. coli* partner protein gave catalytic efficiencies (k_{cat}/K_m for Trx1) which were just a fewfold lower for the heterologous systems compared with the natural systems. The fact that the *H. pylori* TrxR and Trx1 proteins can interact efficiently with the *E. coli* proteins suggests that the *H. pylori* proteins share a great deal of structural similarity with their *E. coli* counterparts and also illustrates the functional homology *H. pylori* Trx1 and TrxR share with other TrxR systems.

To establish the true k_{cat} and K_m values for each substrate of *H. pylori* TrxR, assays varying NADPH at different fixed concentrations of Trx1 were conducted in the absence of additional electron acceptors and were monitored on the stopped-flow spectrophotometer by the time-dependent decrease in NADPH fluorescence. A representative primary Hanes-Wolf plot of the initial-rate data over a range of NADPH concentrations (Fig. 3A) showed that lines representing five different Trx1 concentrations intersected at the *y* axis, denoting a substituted (i.e., ping-pong) reaction mechanism for TrxR (15). The replot of slopes with respect to Trx1 concentration (Fig. 3B) yielded k_{cat} and K_m values, reported in Table 3, which were only slightly different from those for the corresponding *E. coli* proteins. Nonetheless, the catalytic efficiencies (k_{cat}/K_m) of both systems and both substrates are in a similar range, indicating that TrxR and Trx1 act as an effective general protein disulfide reductase system similar to the homologous *E. coli* system.

AhpC cysteine thiol and disulfide quantification. In previous work, our laboratory has demonstrated that peroxidase activity in *S. typhimurium* AhpC is reliant on an essential, conserved cysteine residue (Cys46) while a second active-site cysteine (Cys165′) contributed by a different AhpC subunit stabilizes the oxidized protein through the formation of an intersubunit disulfide bond (21). Thiol quantification of reduced AhpC revealed the presence of two cysteine thiol groups per monomer (2.10 ± 0.17). Denaturation of reduced *H. pylori* AhpC did not change the thiol titer, indicating a high degree of accessibility of the cysteine thiol groups in the reduced protein. As isolated from *E. coli*, overexpressed *H. pylori* AhpC was in its oxidized

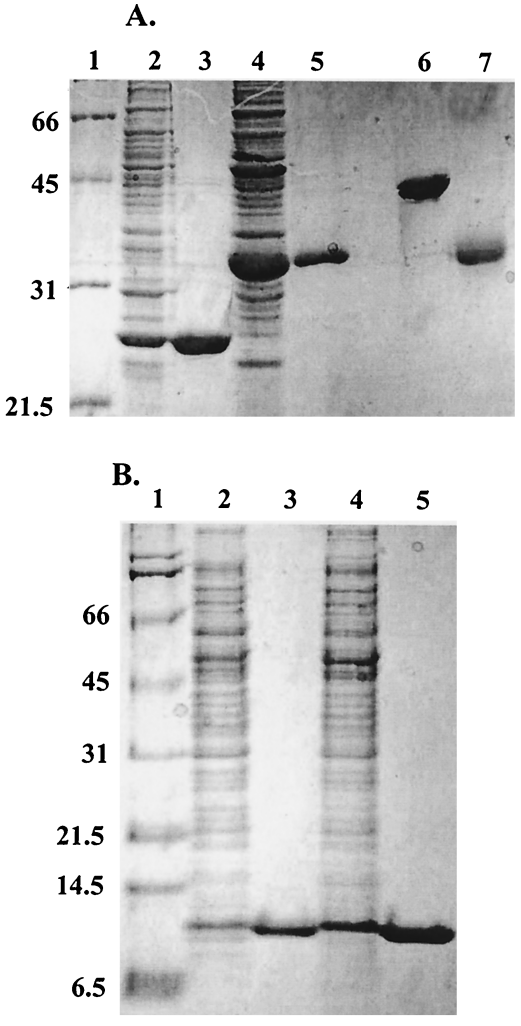

FIG. 1. SDS-PAGE analysis of purified AhpC, Trx1, Trx2, and TrxR from *H. pylori*. (A) Crude lysates and recombinant purified AhpC and TrxR were analyzed on the same 12% polyacrylamide gel in reducing sample buffer (except where noted) as follows: lane 1, molecular mass markers (Broad Range Molecular Weight Standards; Bio-Rad); lane 2, crude extracts of *E. coli* cells transformed with pPROK1/*ahpC* and induced with 0.4 mM IPTG for at least 3 h at 37°C; lane 3, pure, recombinant AhpC; lane 4, crude extracts of *E. coli* cells transformed with pPROK1/*trxR* and induced as described above; lane 5, pure, recombinant TrxR protein; lane 6, pure AhpC in nonreducing sample buffer; lane 7, pure TrxR in nonreducing sample buffer. (B) Crude lysates and recombinant Trx1 and Trx2 were analyzed on a 10% Tris-Tricine gel as follows: lane 1, molecular mass markers; lane 2, crude extracts of *E. coli* cells transformed with pPROK1/*trx1* after induction with IPTG; lane 3, pure, recombinant Trx1; lane 4, crude extracts of *E. coli* cells transformed with pPROK1/*trx2* after induction with IPTG; lane 5, recombinant purified Trx2 after purification. Equivalent protein masses (10 μg) were loaded in all lanes of both gels. Molecular masses (in kilodaltons) are indicated on the left.

form and lacked free thiol groups; NTSB assays revealed that oxidized AhpC contained one disulfide bond per monomer (0.90 ± 0.07). Taken together, along with the presence of intersubunit disulfide bonds in nonreducing SDS-PAGE gels of AhpC (see above), these results support a head-to-tail arrangement of monomers to form two active sites per dimer in *H. pylori* AhpC, as is the case with *S. typhimurium* AhpC.

Peroxidase activity of AhpC, Trx1 or Trx2, and TrxR. To test the ability of *H. pylori* AhpC to reduce hydroperoxides with *H. pylori* Trx1 and TrxR acting as the reducing system, the proteins were mixed with NADPH and cumene hydroperoxide and the change in A_{340} was monitored. The maximal sustained rate of NADPH oxidation was observed when all three proteins, TrxR, Trx1, and AhpC, were included in the assay mixture (Fig. 4). Alone, TrxR possessed oxidase activity (Fig. 4, long, dashed lines), which was observed as a steady decrease in A_{340} at 0.70 s^{-1} in the absence of peroxide; *E. coli* TrxR exhibited a much slower rate of NADPH oxidation (0.01 s^{-1}) under these conditions. In the presence of peroxide, NADPH oxidation by *H. pylori* TrxR alone increased to 0.80 s^{-1}, which is indicative of weak peroxidatic activity of TrxR. In the absence of AhpC, a small burst in NADPH oxidation was first observed (between 0.3 and 1 s) at a rate of 5.1 s^{-1} relative to the TrxR concentration, which tapers off to a rate similar to that of TrxR alone (0.9 s^{-1}) once all of the Trx1 had been reduced (reduction of 5 μM Trx1 accounts for a decrease in A_{340} of 0.03). With all three *H. pylori* proteins present, an initial burst of NADPH oxidation (~6.6 s^{-1} relative to TrxR), at a rate similar to that of TrxR and Trx1 alone, was observed. The somewhat slower but sustained rate observed between 10 and 20 s (2.5 s^{-1}) was not significantly changed when AhpC concentrations were varied, suggesting that both Trx1 reduction by TrxR and AhpC reduction by Trx1 were partially rate limiting under these conditions.

Investigation of the *H. pylori* genome yielded two Trx homologues, Trx1 and Trx2, both of which contain the catalytic WCXXC site required for reductase activity. To determine if Trx2 could act as a reductant for *H. pylori* AhpC, stopped-flow peroxidase experiments in which Trx2 replaced Trx1 in the

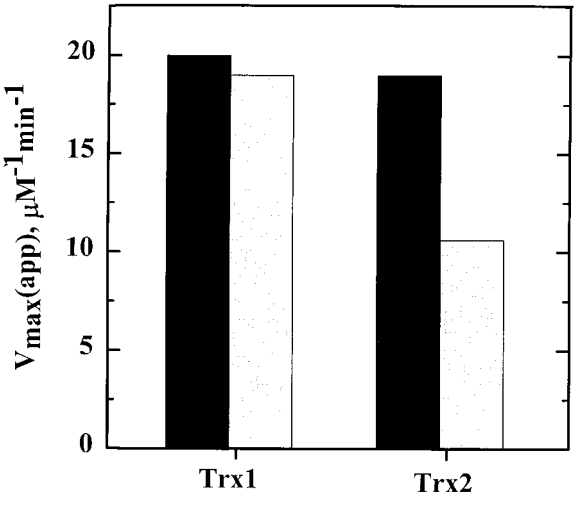

FIG. 2. Comparative kinetic parameters of Trx1 and Trx2 from *H. pylori*. Trx activity assays using either 200 μM DTNB (black bars) or 80 μM insulin (gray bars) as a substrate for 0 to 50 μM Trx1 or Trx2 were conducted in a standard buffer of 100 mM potassium phosphate and 2 mM EDTA, pH 7.4, with 150 μM NADPH. Assays were started with the addition of 7.0 nM TrxR and were monitored at 340 nm when insulin was used as the substrate or at 412 nm when DTNB was used as the substrate to observe the release of TNB^{2-}. Rates were determined from the first 10% of the reaction and then fitted to a hyperbola to determine the V_{max}(app) and K_m(app) values for each.

TABLE 3. Steady-state kinetic parameters of TrxR from *H. pylori* and *E. coli*

TrxR source	k_{cat} (s^{-1})	K_m (μm)		k_{cat}/K_m (M^{-1} s^{-1})	
		NADPH	Trx1	Trx1	NADPH
H. pylori[a]	75	6.1	22.6	3.3×10^6	1.2×10^7
E. coli[b]	33.5	2.7	3.7	9.1×10^6	1.2×10^7

[a] These values were obtained from the slopes and intercepts of the plots in Fig. 3B at 25°C.
[b] These values were obtained from Lennon and Williams (41).

assay mixture were conducted (Fig. 5). Initially, NADPH oxidation rates were quite fast for reactions with Trx2 (6.0 and 14.7 s^{-1} for 5 and 10 μM Trx2, respectively, for data from 0.1 to 1 s), compared to the slower rates occurring at later time points in the same assays (0.8 s^{-1} from 3 to 10 s). After about 5 s, the rates observed for TrxR alone, for TrxR plus 5 μM Trx1, and for AhpC in the presence of TrxR plus 5 or 10 μM Trx2 were all about the same; only the TrxR-Trx1-AhpC system showed a significantly higher sustained rate of NADPH oxidation (Fig. 5). These data indicate that while Trx2 is a good substrate for TrxR, it fails to act as a reductase for *H. pylori* AhpC.

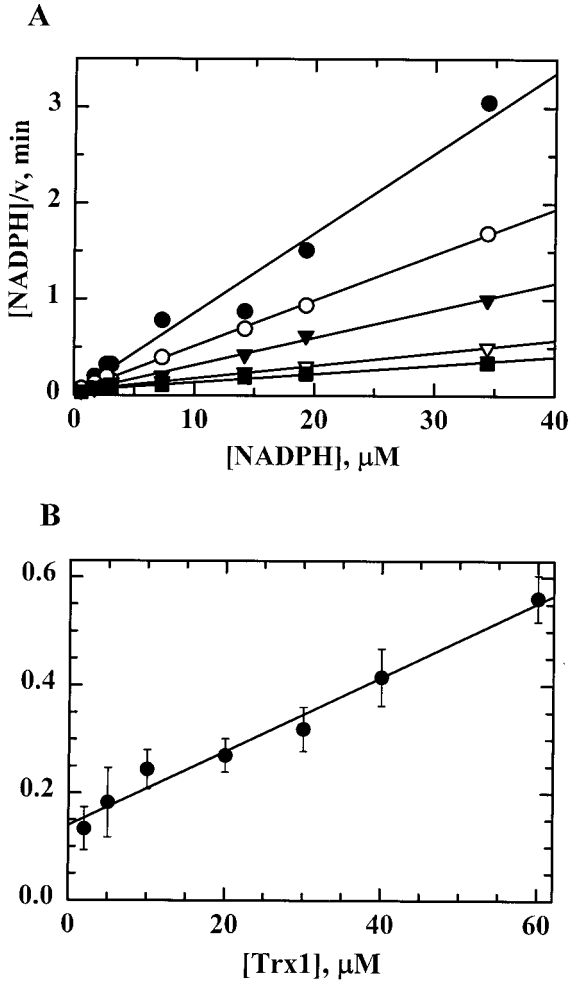

FIG. 3. Steady-state kinetic analysis of Trx1 and TrxR from *H. pylori*. Assays were conducted using a stopped-flow spectrophotometer that monitored the decrease in NADPH fluorescence as described in Materials and Methods. NADPH concentrations (0.8 to 34 μM) were varied at fixed concentrations of Trx1 in the presence of 0.1 μM TrxR. (A) Representative primary Hanes-Wolf plot of one set of initial-rate data for 2 μM (closed circles), 5 μM (open circles), 10 μM (closed triangles), 20 μM (open triangles), and 60 μM (closed squares) Trx1. (B) A replot of the averaged data from three separate experiments was used to calculate the steady-state kinetic parameters for *H. pylori* TrxR as summarized in Table 3.

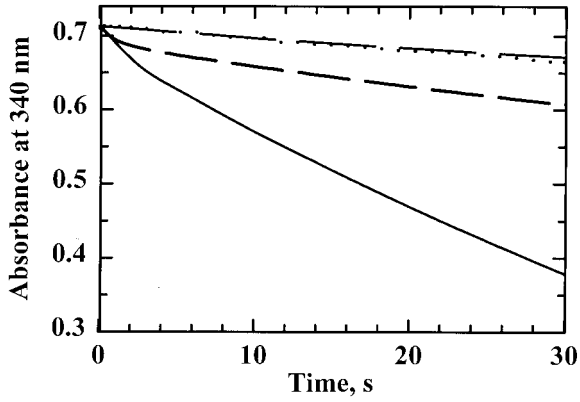

FIG. 4. AhpC activity assays with *H. pylori* AhpC, TrxR, and Trx1. NADPH oxidation was monitored at 340 nm on a stopped-flow spectrophotometer for assay mixtures containing TrxR (0.5 μM), Trx1 (5 μM), and AhpC (20 μM; solid line). Other assays were conducted similarly but in the absence of AhpC (short, dashed line), in the absence of Trx1 (dotted line), or in the absence of both AhpC and Trx1 (long, dashed line). NADPH and CHP (150 μM and 1 mM, respectively, after mixing) were incubated in one syringe with peroxidase assay buffer, and assays were initiated when substrates were mixed with proteins incubated in the second syringe with peroxidase buffer.

Proof that AhpC reduces peroxides was obtained using an endpoint assay in which the peroxide concentration was monitored over the course of the incubation. In an assay mixture containing TrxR, Trx1, AhpC, NADPH, and H_2O_2, ferrithiocyanate complex formation with H_2O_2 decreased over time (5.0 s^{-1} relative to TrxR), indicating that peroxide was continually consumed in the presence of *H. pylori* AhpC (Fig. 6). When AhpC was not included in the reaction mixture, no decrease in the peroxide levels was observed. Again, reaction rates were not linear with respect to AhpC concentrations due to partially rate-limiting reduction by TrxR and Trx1 (data not shown). Full kinetic characterization of AhpC with its reducing system TrxR-Trx1 is described in a later section.

Specificity of *H. pylori* AhpC for TrxR-Trx1 or AhpF-like reductase systems. In *S. typhimurium* and most other bacterial systems, the AhpC component is reduced by a specialized flavoprotein related to TrxR and known as AhpF, NADH oxidase, Nox-1, or PrxR (55). In a set of experiments designed to test the specificity of *H. pylori* AhpC for its own reductase system, *S. typhimurium* AhpF replaced *H. pylori* Trx1 and TrxR in the stopped-flow peroxidase assay mixture with *H. pylori* AhpC. No significant rate of NADH oxidation was observed in an anaerobic *S. typhimurium* AhpF and *H. pylori* AhpC system (Fig. 5, medium dashes). Higher concentrations of AhpF still showed no activity with *H. pylori* AhpC (data not shown), indicating a clear specificity of the cysteine-based peroxidase for reduction by Trx1 rather than by AhpF from a different bacterial source. *S. typhimurium* AhpC (10 μM) also exhibited

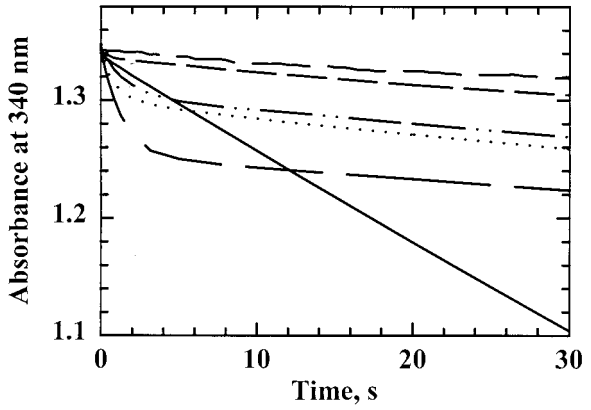

FIG. 5. AhpC activity assay with Trx1 or Trx2 as the reductant. The decrease in NADPH absorbance was monitored on a stopped-flow spectrophotometer when AhpC (20 μM) and TrxR (0.5 μM) were assayed with Trx1 (5.0 μM, solid line) or with Trx2 (5.0 μM, dotted line; 10 μM, long dashes) in peroxidase assay buffer as described in the legend to Fig. 4. Assays of TrxR-Trx1 excluding the AhpC protein (dashed-dotted line) and assays of TrxR alone (small dashes) were also conducted. AhpF (0.5 μM) from *S. typhimurium* was included in place of TrxR-Trx1 with *H. pylori* AhpC (medium dashes), and in this case, NADH rather than NADPH was used as the reducing substrate under anaerobic conditions.

considerable specificity for its own reductase, AhpF (0.5 μM), compared with reduction by *E. coli* TrxR (0.5 μM) plus *E. coli* Trx1 (5 μM); turnover rates were 42 s^{-1} with AhpF and 1.7 s^{-1} with *E. coli* TrxR-Trx1 (data not shown). Nonetheless, the rate of turnover of *S. typhimurium* AhpC with the *E. coli* TrxR-Trx1 system was only about twofold lower than that of *H. pylori* AhpC with its own TrxR-Trx1 system (3.2 s^{-1} under the same conditions) while *H. pylori* AhpC and *S. typhimurium* AhpF interaction was undetectable. Among the proteins under investigation, *H. pylori* TrxR and Trx1 and *E. coli* TrxR and Trx1 were the most interchangeable in peroxidase assays. *H. pylori* AhpC (2 μM) assayed with the *E. coli* proteins TrxR (2 μM) and Trx1 (25 μM) exhibited a rate of NADPH oxidation that was about the same as that obtained with *H. pylori* TrxR-Trx1 under the same conditions (1.9 versus 3.2 s^{-1}).

Steady-state kinetics of AhpC. To further investigate the peroxidase activity of *H. pylori* AhpC, reaction conditions were first established under which initial rates were directly proportional to AhpC at a Trx1 concentration (30 μM) that was at least 10-fold higher than the maximal concentration of AhpC (3 μM). Because the very low intrinsic NADPH oxidase activity of *E. coli* TrxR allowed the observation of low peroxidase rates above background NADPH turnover, *E. coli* TrxR replaced *H. pylori* TrxR using concentrations that were high enough (2 to 3 μM) to support rapid *H. pylori* Trx1 recycling (i.e., additional TrxR did not further increase observed rates of NADPH oxidation). AhpC-dependent rates of NADPH oxidation measured over a range of Trx1 concentrations (15 to 30 μM) suggested a simple bimolecular interaction between reduced Trx1 and oxidized AhpC at a rate of 1.0×10^5 M^{-1} s^{-1} (data not shown).

Given the putative nonsaturable interaction between Trx1 and AhpC suggested by the studies described above and the need for information concerning interactions between reduced AhpC and hydroperoxide substrates, kinetic data were generated and analyzed as described previously by Dalziel (18). Because the secondary Dalziel plots (e.g., Fig. 7B) intersect the *y* axis at the origin (within experimental error), the K_m values of AhpC for peroxides and Trx1 and V_{max} values are infinite. Parallel lines in the primary plot (Fig. 7A) also indicate a substituted (ping-pong) mechanism for *H. pylori* AhpC by which AhpC does not form detectable enzyme-substrate complexes with either substrate and displays nonsaturating kinetics, a kinetic pattern that has been observed for other nonheme peroxidases, such as glutathione peroxidase (23) and tryparedoxin peroxidase (46).

With the above observations in mind, the rate data were plotted using the Dalziel equation for two-substrate reactions in which enzyme-substrate complexes are not observed: $[E]_0/v = \phi_1/[\mathrm{ROOH}] + \phi_2/[\mathrm{Trx1}]$, where $[E]$ is the concentration of AhpC and ϕ_1 and ϕ_2 are the Dalziel kinetic coefficients. Because enzyme-substrate complexes are not observed experimentally, the interactions of AhpC with its two substrates can be depicted as a sequence of consecutive, bimolecular, nonreversible reactions: $\mathrm{AhpC_{red}} + \mathrm{ROOH} \rightarrow \mathrm{AhpC_{ox}} + \mathrm{ROH} + \mathrm{H_2O}$ and $\mathrm{AhpC_{ox}} + \mathrm{TrxR_{ed}} \rightarrow \mathrm{AhpC_{red}} + \mathrm{Trx1_{ox}}$. The apparent limiting rates for these two reactions are characterized by their kinetic rate constants, k_1' and k_2', respectively, which are the reciprocals of the Dalziel coefficients, ϕ_1 and ϕ_2. To obtain the rate constants, the rate data were evaluated using the integrated Dalziel equation (24). After elucidating product and reactant amounts at various times, the data were substituted into the integrated rate equation (given in Materials and Methods) and plotted (Fig. 7A). The slopes of the lines in the primary plot are equal to ϕ_1: *y* intercepts from Fig. 7A replotted in Fig. 7B versus the reciprocal of the Trx1 concentration produced a line with a slope of ϕ_2. By taking the reciprocal of ϕ_2, the second-order rate constant, k_2', of 1.0×10^5 M^{-1} s^{-1} was determined for the interaction between AhpC and Trx1, giving the same value as that obtained using the AhpC-dependent assays described above, in which the peroxide substrate

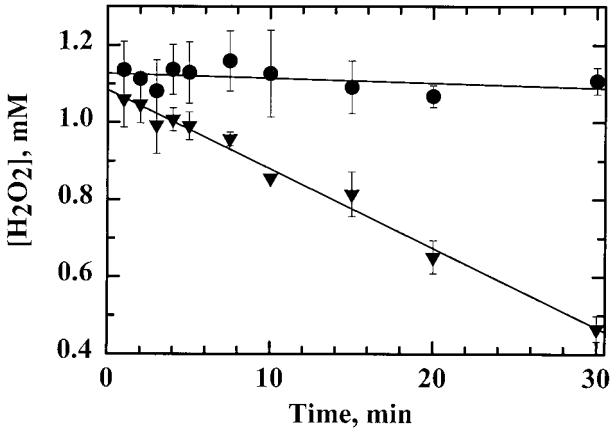

FIG. 6. Peroxide consumption by *H. pylori* AhpC. The disappearance of peroxide was monitored by ferrithiocyanate complex formation following incubations of a mixture containing 20 μM AhpC (triangles) or 0 μM AhpC (circles) with TrxR (0.2 μM), Trx1 (2.0 μM), and an NADPH-regenerating system consisting of glucose-6-phosphate (10 mM), glucose-6-phosphate dehydrogenase (0.2 U/ml), and NADPH (10 μM) in 500-μl volumes. All reactions were started with the addition of H_2O_2 (1 mM) as described in Materials and Methods.

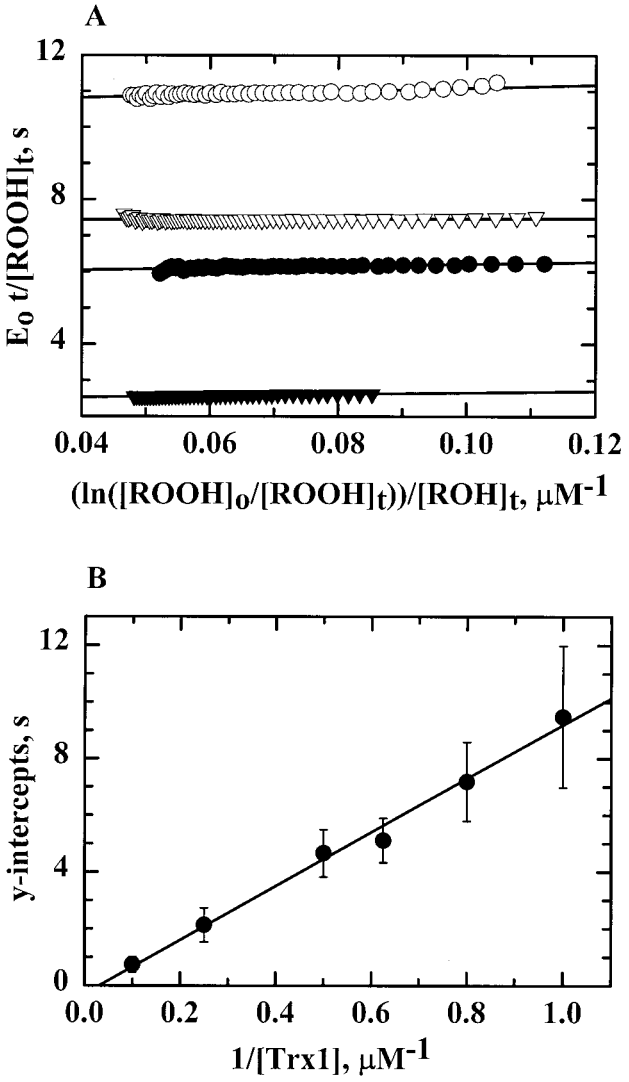

FIG. 7. Kinetic analysis of AhpC from *H. pylori* by the Dalziel method. Assays of AhpC were conducted on a stopped-flow spectrophotometer using AhpC (4.0 μM), Trx1 (2.0 μM), and *E. coli* TrxR (1.0 μM) with NADPH (150 μM) and limiting amounts of peroxide (10 to 40 μM). Proteins were incubated with NADPH for 5 min prior to mixing with peroxide. The resulting reaction traces were used to calculate [ROOH] and [ROH] over time. (A) In the Dalziel primary plot, a least-squares linear regression line was obtained for the calculated data points for five different concentrations of Trx1: 4.0 μM (closed triangles), 2.0 μM (closed circles), 1.6 μM (open triangles), and 1.0 μM (open circles). The resulting lines give slopes of ϕ_1 and intercepts of ϕ_2/[Trx1]. (B) The apparent maximum velocities (*y* intercepts from the primary plot) were replotted in a Dalziel secondary plot against the reciprocal of the [Trx1] at which they were obtained. The slope of the resulting linear regression line is ϕ_2.

was in excess. Using a similar strategy, the value for k_1' (2.0×10^5 M^{-1} s^{-1}) was determined for the interaction of AhpC with H_2O_2 and was of a magnitude similar to that of k_2' for the oxidation of Trx1. Therefore, both steps are partially rate limiting under these conditions.

AhpC was also tested for the ability to reduce peroxides other than H_2O_2, including EtOOH, *t*-BOOH, CHP, and linoleic acid hydroperoxide (LOOH). Using one concentration of Trx1 (2.0 μM), the slopes from the primary plot were determined for each peroxide to yield the following apparent k_1' values: H_2O_2, 2.0×10^5 M^{-1} s^{-1}; EtOOH, 1.7×10^5 M^{-1} s^{-1}; *t*-BOOH, 1.6×10^5 M^{-1} s^{-1}; CHP, 1.2×10^5 M^{-1} s^{-1}; LOOH, 1.1×10^5 M^{-1} s^{-1}. AhpC was capable of reducing the different peroxides, including the more structurally complex compounds *t*-BOOH and LOOH, with similar apparent rate constants. No change in k_2' reflecting the interaction between Trx1 and AhpC was observed for the different hydroperoxide substrates.

Essentiality of *H. pylori ahpC*. Allelic replacement mutagenesis of *ahpC* was conducted to study the physiological role of AhpC in *H. pylori* and to determine the effect of AhpC removal on *H. pylori*'s responses to oxidative stress. When *ahpC* interrupted with the *camR* cassette was introduced into *H. pylori* strains HP26695, SS1, HP1061, and HP1, there was no growth of colonies on selective medium after 7 days of incubation, whereas a few thousand colonies are normally obtained after 2 to 3 days for nonessential-gene knockouts carried out in this manner (e.g., with the *rdxA* knockout control). While single crossover events have been described in *H. pylori* using this method of transformation (57), no such phenomenon was observed even after several repeated transformation attempts. A similar construct was successfully generated in which the nitroreductase (*rdxA*) gene was knocked out with the same *camR* cassette (26) and introduced by transformation and homologous recombination into the same *H. pylori* strains. Both Cam^r and Mtz^r (metronidazole-resistant) colonies were formed, indicating that *rdx* is not essential for growth. Therefore, the loss of growth under microaerobic conditions with the loss of *ahpC* strongly suggests an essential role for AhpC in *H. pylori* viability.

Genetic characterization of *ahpC*. The gene encoding AhpC is located between *ceuE* (HP1562, encoding an iron III ABC transporter) transcribed in the opposite direction and a gene encoding an outer membrane protein (HP1564) in the same orientation as *ahpC* and containing endogenous promoter sequences (71). The location of the transcriptional start site of *ahpC* was determined by primer extension analysis. Two prominent reverse transcript bands migrate parallel to G and T residues, 96 and 94 bp upstream, respectively, from the AUG translation initiation codon (Fig. 8A). Sequences resembling the *H. pylori* σ^{70} consensus sequence (25) were located at the expected distance from the transcriptional start site (Fig. 8B, bold). The potential −10 hexamer of the putative *ahpC* promoter, TATACT, displays a high degree of identity (5 of 6 bp) to the −10 consensus sequence for *H. pylori*, TAtaaT (25). Other putative regulatory sequence elements were identified in the promoter region centered around −40 and +10 (underlined, Fig. 8B), underscoring the possibility that *ahpC* transcription is regulated. However, no Fur (ferric uptake regulator) binding site (69) was evident in the *H. pylori ahpC* promoter region and the *H. pylori* genome lacks a structural gene for OxyR, the redox-sensitive transcription factor which upregulates AhpC production in response to oxidative stress in other eubacteria (65). Although the deduced *H. pylori* AhpC amino acid sequence has already been published, the protein was not identified as an alkyl hydroperoxide reductase and the translational start site of *ahpC* was not correctly positioned by O'Toole et al. (48).

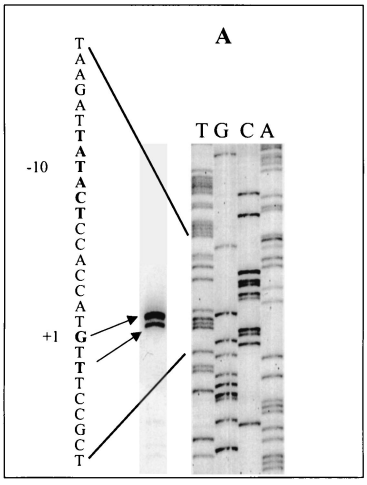

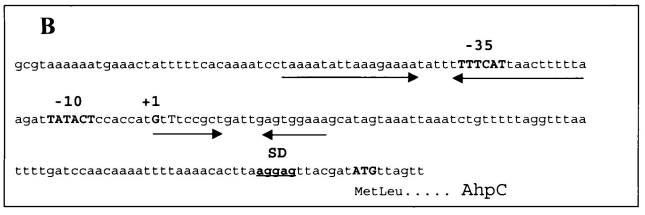

FIG. 8. Primer extension analysis of *ahpC*. (A) To map the transcriptional start site of *H. pylori* AhpC mRNA, a [$\gamma-^{32}$P]ATP-labeled oligonucleotide complementary to the 5′ end of *ahpC* was hybridized to 100 μg of total RNA and extended using reverse transcriptase. DNA sequencing reactions carried out with the same primer (right) were electrophoresed concomitantly with the primer extension products (left) to the left on a 6% urea polyacrylamide sequencing gel. Two potential 5′ ends of the *ahpC* transcript are 96 (G) and 94 (T) bp upstream from the AUG translation initiation codon. The potential −10 hexamer of the putative *ahpC* promoter is indicated in bold upstream of the transcriptional start site. (B) Shown is the DNA sequence of the region upstream of *ahpC* from *H. pylori* strain 26695. The potential *ahpC* transcription and translation start signals are shown in bold, as well as the Shine-Dalgarno (SD) ribosome binding site and the putative promoter sites centered at −10 and −35. The inverted repeats are indicated by arrows.

DISCUSSION

Antioxidant systems critical to the defense of *H. pylori* against ROS generated by the oxidative burst of macrophages and polymorphonuclear leukocytes are central to the ability of this organism to establish chronic infections in gastric tissues and to combat the high degree of inflammatory responses mounted by the host. To date, Fe-dependent superoxide dismutase (63), catalase (47), and the Trx-dependent peroxidase (AhpC) described herein have been characterized as *H. pylori* antioxidant enzymes. Deletion of the gene encoding catalase (*katA*) from the *H. pylori* chromosome did not affect the viability of the organism (71), whereas we have found that *ahpC* is essential for *H. pylori* survival under microaerobic conditions. Previous studies with other organisms in which the *ahpC* locus was deleted or mutated have not demonstrated AhpC essentiality. For example, in studies of the closely related, but more aerotolerant, enteric pathogen *C. jejuni*, deletion of *sodB* decreased its capacity to survive in macrophages (50), while deletion of *ahpC* increased susceptibility to oxidative stress (4); nonetheless, viability under conditions of low oxygen tension was not affected for either mutant. In support of our findings, two other groups have recently reported attempts to knock out *H. pylori ahpC* and have reached similar conclusions regarding its essentiality (42, 13). *H. pylori* sensitivity toward oxidative damage is highlighted by its dependence on microaerophilic growth conditions. Its inability to grow in the absence of *ahpC* is a clear reflection of the delicate redox balance required to support, yet not inactivate, key metabolic enzymes (37).

Given the apparent requirement of TrxR-Trx1 for AhpC activity, the TrxR-Trx1 reductase system is also likely to be indispensable for *H. pylori* viability, as well, although this hypothesis has yet to be tested. The alternative, that an as-yet-unidentified reductase is also capable of AhpC reduction, is also a possibility. Interestingly, no homologues for the *E. coli* glutathione reductase system, such as glutaredoxin (*grxA*), γ-L-glutamyl-L-cysteine synthetase (*gshA*), or glutathione reductase (*gorA*), can be found in the *H. pylori* genome. Therefore, *H. pylori* does not have the main other reductase system that can serve as a compensatory mechanism in most other organisms (56), highlighting the possible fundamental requirement for a functional TrxR-Trx1 system in *H. pylori*.

Our demonstration that the 26-kDa protein previously described as an abundant "species-specific antigen" by O'Toole et al. (48) is a cysteine-based peroxidase reactivated by reduced Trx agrees nicely with the sequence-based comparisons of *H. pylori* AhpC with a wide variety of other Prxs. A subset of these proteins, some of which have been classified as TPxs, are not reducible by bacterial AhpF proteins and rely on reducing equivalents from Trx to support turnover with cellular peroxides (10, 33, 36, 52). We have found that this capacity to accept electrons from reduced Trx is a property common to bacterial AhpC proteins as well, which nonetheless show much greater reactivity toward their specialized flavoprotein reductase, AhpF. Some eukaryotic Prxs, on the other hand, are incapable of turnover with reduced Trx proteins, at least under the conditions tested (22, 35). The specificity of such cysteine-based peroxidases for reduced Trx, as implied by the TPx designation, is therefore of questionable validity as a unique functional description distinguishing this group among the diverse Prx proteins.

In cases in which the reactivation of Prx proteins by their electron donor proteins has been investigated in detail, two different kinetic patterns have been observed. For AhpF-AhpC interactions, reduction of AhpC by AhpF is a saturable phenomenon characterized by a K_m for AhpC of around 15 μM and a k_{cat}/K_m for the flavoprotein of $\sim 10^7$ M^{-1} s^{-1} (55). For the Prx system from *C. fasciculata*, interaction of reduced tryparedoxin with its peroxidase is a bimolecular process with infinite k_{cat} and K_m values and a second-order rate constant of 1.5×10^6 to 3.5×10^6 M^{-1} s^{-1} (46). Here, we have demonstrated that the interaction of Trx1 with *H. pylori* AhpC is also bimolecular ($\sim 10^5$ M^{-1} s^{-1}) and that therefore no enzyme-substrate complexes between Trx1 and AhpC can be detected kinetically. Presumably, this kinetic pattern will hold for other Trx-dependent Prx proteins as well when such kinetic profiles are investigated.

Using kinetic studies akin to those previously applied to another Prx, tryparedoxin peroxidase from *C. fasciculata*, the interaction of *H. pylori* AhpC with peroxides was also shown to be a bimolecular process (like Trx-Prx interactions) lacking

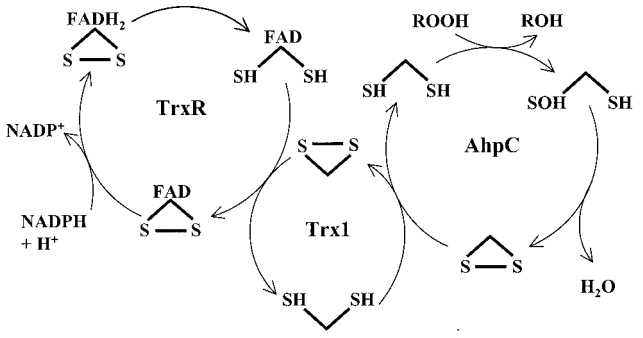

FIG. 9. Pathway for transfer of reducing equivalents from NADPH to hydroperoxide in the alkyl hydroperoxide reductase system from *H. pylori*. Note that the enzyme species shown do not necessarily represent actual catalytic intermediates. FAD, flavin adenine dinucleotide.

detectable enzyme-substrate complexes. This ping-pong mechanism has also been observed for the distantly related glutathione peroxidases (23, 68). The higher rate of enzyme-peroxide interaction for glutathione peroxidase ($\sim 10^8$ M^{-1} s^{-1}) has been attributed to the unique reactivity of the selenocysteine at the active site (64), although at 10^5 to 10^6 M^{-1} s^{-1}, the rate of peroxide reduction is still quite high and indicative of an important role for *H. pylori* AhpC in cellular peroxide metabolism. Using k_1' to characterize the protein-peroxide interaction, our experiments demonstrated essentially no specificity when AhpC was tested with a wide variety of small, bulky, aromatic, or lipid hydroperoxide substrates, as was true of the *C. fasciculata* peroxidase (46). Differential reactivities toward particular hydroperoxide substrates have been reported for some other Prx enzymes based on less quantitative analyses (9, 33, 34). In addition, peroxynitrite ($OONO^-$) has recently been shown to be a substrate for *H. pylori* AhpC, with the rate of decomposition occurring at a second-order rate constant of 1.21×10^6 M^{-1} s^{-1} (7). These results are all consistent with a minimal binding site on AhpC for hydroperoxides (and peroxynitrite) consisting of little more than the catalytic residue (Cys49) at the active site.

On the basis of results reported here and mechanisms outlined for other 2-Cys AhpC homologues (10, 51), electrons from NADPH proceed along the path outlined in Fig. 9 for the reduction of peroxides to alcohols. This scheme is highly analogous to that for electron transfer through the *S. typhimurium* AhpC system, except that TrxR and Trxl replace AhpF in the *H. pylori* system. Nonetheless, one tightly bound flavin and three disulfide redox centers mediate electron transfer from pyridine nucleotide to peroxide in both cases.

Little information exists on potential redox or iron regulation of *H. pylori* AhpC expression, although in other studies of TrxR and Trx1 from *H. pylori*, Windle et al. (74) observed that Trxl expression dramatically increased under conditions of oxidative stress; Trx1 was therefore classified as a stress response element in *H. pylori*. While the proximal location of *trxR* and *trx1* in the chromosome could provide the bacterium with a mechanism for a coordinated response eliciting expression of both proteins, an increase in TrxR expression did not accompany increased Trx1 expression under oxidative stress conditions (74). Interestingly, reductase activity of the TrxR-Trx1 reductase system was also reportedly present in the media of culture supernatants and could be available to support extracellular peroxide reduction by AhpC if the latter protein is also exported.

In conclusion, this is the first report of a Trx-dependent alkyl hydroperoxide system from a gastric pathogen. To our knowledge, AhpC from *H. pylori* is only the second known bacterial AhpC to be demonstrated experimentally to require the Trx-reducing system for reduction of the oxidized AhpC active site. An essential role for AhpC in *H. pylori* has been established with our *ahpC* mutagenesis experiments, and this is, to our knowledge, the only case in which an *ahpC* locus has been shown to be required for viability. The presence of this essential Trx-dependent peroxidase in *H. pylori* suggests important roles for TrxR, Trx1, and AhpC in the removal of alkyl hydroperoxides to protect against oxidative stress and in the preservation of the microaerobic environment required for *H. pylori* viability.

ACKNOWLEDGMENTS

Funding for this work was provided in part by grants from the National Institutes of Health (NIH R01 GM50389) to L.B.P. and from the Canadian Institutes for Health Research (CIHR MT11318 and RP14292) to P.S.H.

We are particularly grateful to C. M. Reynolds for the purification of *E. coli* Trx1 and TrxR and to Desnee Wynn, Lois LaPrade, and Louis Bryden for technical assistance. Special thanks to Joseph O'Flaherty for his assistance with the fatty acid hydroperoxide preparation and to James Luba for helpful discussions of the kinetic data.

REFERENCES

1. **Alphey, M. S., C. S. Bond, E. Tetaud, A. H. Fairlamb, and W. N. Hunter.** 2000. The structure of reduced tryparedoxin peroxidase reveals a decamer and insight into reactivity of 2-Cys peroxiredoxins. J. Mol. Biol. **300:**903–916.
2. **Altschul, S. F., W. Gish, W. Miller, E. W. Myers, and D. J. Lipman.** 1990. Basic local alignment search tool. J. Mol. Biol. **215:**403–410.
3. **Ausubel, F. M., R. B. Brent, R. E. Kingston, D. D. Moore, J. G. Seidman, J. A. Smith, and K. Struhl (ed.).** 1999. Short protocols in molecular biology. John Wiley & Sons, Inc., New York, N.Y.
4. **Baillon, M. L., A. H. van Vliet, J. M. Ketley, C. Constantinidou, and C. W. Penn.** 1999. An iron-regulated alkyl hydroperoxide reductase (AhpC) confers aerotolerance and oxidative stress resistance to the microaerophilic pathogen *Campylobacter jejuni*. J. Bacteriol. **181:**4798–4804.
5. **Baker, L. M. S., and L. B. Poole.** 1999. An alkyl hydroperoxide reductase system from the gastric pathogen, *Helicobacter pylori*: cloning, purification, and kinetic studies. FASEB J. **13:**A1447.
6. **Baker, L. M. S., and L. B. Poole.** 2000. Thioredoxin 1, not Thioredoxin 2, selectively reduces the peroxidase component of *Helicobacter pylori's* alkyl hydroperoxide reductase system. FASEB J. **14:**A1525.
7. **Bryk, R., P. Griffin, and C. Nathan.** 2000. Peroxynitrite reductase activity of bacterial peroxiredoxins. Nature. **407:**211–215.
8. **Buck, G. K., W. K. Gourley, W. K. Lee, K. Subramanyam, J. M. Latimer, and A. R. DiNuzzo.** 1986. Relation of *Campylobacter pyloridis* to gastritis and peptic ulcer. J. Infect. Dis. **153:**664–669.
9. **Cha, M. K., C. H. Yun, and I. H. Kim.** 2000. Interaction of human thiol-specific antioxidant protein 1 with erythrocyte plasma membrane. Biochemistry **39:**6944–6950.
10. **Chae, H. Z., S. J. Chung, and S. G. Rhee.** 1994. Thioredoxin-dependent peroxide reductase from yeast. J. Biol. Chem. **269:**27670–27678.
11. **Chae, H. Z., S. W. Kang, and S. G. Rhee.** 1999. Isoforms of mammalian peroxiredoxin that reduce peroxides in presence of thioredoxin. Methods Enzymol. **300:**219–226.
12. **Chae, H. Z., K. Robinson, L. B. Poole, G. Church, G. Storz, and S. G. Rhee.** 1994. Cloning and sequencing of thiol-specific antioxidant from mammalian brain: alkyl hydroperoxide reductase and thiol-specific antioxidant define a large family of antioxidant enzymes. Proc. Natl. Acad. Sci. USA **91:**7017–7021.
13. **Chalker, A. F., H. W. Minehart, N. J. Hughes, K. K. Koretke, M. A. Lonetto, K. K. Brinkman, P. V. Warren, A. Lupas, M. J. Stanhope, J. R. Brown, and P. S. Hoffman.** 2001. Systematic identification of selective genes in *Helicobacter pylori* by genome prioritization and allelic replacement mutagenesis. J. Bacteriol. **183:**1259–1268.
14. **Cohen, G., M. Yanko, M. Mislovati, A. Argaman, R. Schreiber, Y. Av-Gay, and Y. Aharonowitz.** 1993. Thioredoxin-thioredoxin reductase system of *Strep-*

tomyces clavuligerus: sequences, expression, and organization of the genes. J. Bacteriol. **175:**5159–5167.
15. **Cornish-Bowden, A.** 1999. Fundamentals of enzyme kinetics. Portland Press, Ltd., London, England.
16. **Correa, P.** 1995. *Helicobacter pylori* and gastric carcinogenesis. Am. J. Surg. Pathol. **19:**S37–S43.
17. **Correa, P.** 1988. A human model of gastric carcinogenesis. Cancer Res. **48:** 3554–3560.
18. **Dalziel, K.** 1957. Initial steady state velocities in the evaluation of enzyme-coenzyme-substrate reaction mechanisms. Acta Chem. Scand. **11:**1706–1723.
19. **Davies, G. R., N. J. Simmonds, T. R. Stevens, M. T. Sheaff, N. Banatvala, I. F. Laurenson, D. R. Blake, and D. S. Rampton.** 1994. *Helicobacter pylori* stimulates antral mucosal reactive oxygen metabolite production *in vivo*. Gut **35:**179–185.
20. **Ellis, H. R., and L. B. Poole.** 1997. Novel application of 7-chloro-4-nitrobenzo-2-oxa-1,3-diazole to identify cysteine sulfenic acid in the AhpC component of alkyl hydroperoxide reductase. Biochemistry **36:**15013–15018.
21. **Ellis, H. R., and L. B. Poole.** 1997. Roles for the two cysteine residues of AhpC in catalysis of peroxide reduction by alkyl hydroperoxide reductase from *Salmonella typhimurium*. Biochemistry **36:**13349–13356.
22. **Fisher, A. B., C. Dodia, Y. Manevich, J. W. Chen, and S. I. Feinstein.** 1999. Phospholipid hydroperoxides are substrates for non-selenium glutathione peroxidase. J. Biol. Chem. **274:**21326–21334.
23. **Flohe, L., G. Loschen, W. A. Gunzler, and E. Eichele.** 1972. Glutathione peroxidase. V. The kinetic mechanism. Hoppe Seyler's Z. Physiol. Chem. **353:**987–999.
24. **Forstrom, J. W., F. H. Stults, and A. L. Tappel.** 1979. Rat liver cytosolic glutathione peroxidase: reactivity with linoleic acid hydroperoxide and cumene hydroperoxide. Arch. Biochem. Biophys. **193:**51–55.
25. **Forsyth, M. H., and T. L. Cover.** 1999. Mutational analysis of the *vacA* promoter provides insight into gene transcription in *Helicobacter pylori*. J. Bacteriol. **181:**2261–2266.
26. **Goodwin, A., D. Kersulyte, G. Sisson, S. J. Veldhuyzen van Zanten, D. E. Berg, and P. S. Hoffman.** 1998. Metronidazole resistance in *Helicobacter pylori* is due to null mutations in a gene (*rdxA*) that encodes an oxygen-insensitive NADPH nitroreductase. Mol. Microbiol. **28:**383–393.
27. **Graham, D. Y., and P. D. Klein.** 1987. *Campylobacter pyloridis* gastritis: the past, the present, and speculations about the future. Am. J. Gastroenterol. **82:**283–286.
28. **Guruge, J. L., P. G. Falk, R. G. Lorenz, M. Dans, H. P. Wirth, M. J. Blaser, D. E. Berg, and J. I. Gordon.** 1998. Epithelial attachment alters the outcome of *Helicobacter pylori* infection. Proc. Natl. Acad. Sci. USA **95:**3925–3930.
29. **Holmgren, A.** 1968. Thioredoxin. 6. The amino acid sequence of the protein from *Escherichia coli B.* Eur. J. Biochem. **6:**475–484.
30. **Holmgren, A., and M. Bjornstedt.** 1995. Thioredoxin and thioredoxin reductase. Methods Enzymol. **252:**199–306.
31. **Holmgren, A., and P. Reichard.** 1967. Thioredoxin. 2. Cleavage with cyanogen bromide. Eur. J. Biochem. **2:**187–196.
32. **Jacobson, F. S., R. W. Morgan, M. F. Christman, and B. N. Ames.** 1989. An alkyl hydroperoxide reductase from *Salmonella typhimurium* involved in the defense of DNA against oxidative damage. Purification and properties. J. Biol. Chem. **264:**1488–1496.
33. **Jeong, J. S., S. J. Kwon, S. W. Kang, S. G. Rhee, and K. Kim.** 1999. Purification and characterization of a second type thioredoxin peroxidase (type II TPx) from *Saccharomyces cerevisiae*. Biochemistry **38:**776–783.
34. **Jeong, W., M. K. Cha, and I. H. Kim.** 2000. Thioredoxin-dependent hydroperoxide peroxidase activity of bacterioferritin comigratory protein (BCP) as a new member of the thiol-specific antioxidant protein (TSA)/alkyl hydroperoxide peroxidase C (AhpC) family. J. Biol. Chem. **275:**2924–2930.
35. **Kang, S. W., I. C. Baines, and S. G. Rhee.** 1998. Characterization of a mammalian peroxiredoxin that contains one conserved cysteine. J. Biol. Chem. **273:**6303–6311.
36. **Kang, S. W., H. Z. Chae, M. S. Seo, K. Kim, I. C. Baines, and S. G. Rhee.** 1998. Mammalian peroxiredoxin isoforms can reduce hydrogen peroxide generated in response to growth factors and tumor necrosis factor-alpha. J. Biol. Chem. **273:**6297–6302.
37. **Kelly, D. J.** 1998. The physiology and metabolism of the human gastric pathogen *Helicobacter pylori*. Adv. Microb. Physiol. **40:**137–189.
38. **Kitano, K., Y. Niimura, Y. Nishiyama, and K. Miki.** 1999. Stimulation of peroxidase activity by decamerization related to ionic strength: AhpC protein from *Amphibacillus xylanus*. J. Biochem. (Tokyo) **126:**313–319.
39. **Klenk, H. P., R. A. Clayton, J. F. Tomb, O. White, K. E. Nelson, K. A. Ketchum, R. J. Dodson, M. Gwinn, E. K. Hickey, J. D. Peterson, D. L. Richardson, A. R. Kerlavage, D. E. Graham, N. C. Kyrpides, R. D. Fleischmann, J. Quackenbush, N. H. Lee, G. G. Sutton, S. Gill, E. F. Kirkness, B. A. Dougherty, K. McKenney, M. D. Adams, B. Loftus, J. C. Venter et al.** 1997. The complete genome sequence of the hyperthermophilic, sulphate-reducing archaeon *Archaeoglobus fulgidus*. Nature **390:**364–370.
40. **Lee, A., J. O'Rourke, M. C. De Ungria, B. Robertson, G. Daskalopoulos, and M. F. Dixon.** 1997. A standardized mouse model of *Helicobacter pylori* infection: introducing the Sydney strain. Gastroenterology **112:**1386–1397.
41. **Lennon, B. W., and C. H. Williams, Jr.** 1997. Reductive half-reaction of thioredoxin reductase from *Escherichia coli*. Biochemistry **36:**9464–9477.
42. **Lundstrom, A. M., and I. Bolin.** 2000. A 26 kDa protein of *Helicobacter pylori* shows alkyl hydroperoxide reductase (AhpC) activity and the mono-cistronic transcription of the gene is affected by pH. Microb. Pathog. **29:**257–266.
43. **Maiorino, M., C. Gregolin, and F. Ursini.** 1990. Phospholipid hydroperoxide glutathione peroxidase. Methods Enzymol. **186:**448–457.
44. **Mallett, T. C., and A. Claiborne.** 1998. Oxygen reactivity of an NADH oxidase C42S mutant: evidence for a C(4a)-peroxyflavin intermediate and a rate-limiting conformational change. Biochemistry **37:**8790–8802.
45. **Miranda-Vizuete, A., A. E. Damdimopoulos, J. Gustafsson, and G. Spyrou.** 1997. Cloning, expression, and characterization of a novel *Escherichia coli* thioredoxin. J. Biol. Chem. **272:**30841–30847.
46. **Nogoceke, E., D. U. Gommel, M. Kiess, H. M. Kalisz, and L. Flohe.** 1997. A unique cascade of oxidoreductases catalyses trypanothione-mediated peroxide metabolism in *Crithidia fasciculata*. Biol. Chem. **378:**827–836.
47. **Odenbreit, S., B. Wieland, and R. Haas.** 1996. Cloning and genetic characterization of *Helicobacter pylori* catalase and construction of a catalase-deficient mutant strain. J. Bacteriol. **178:**6960–6967.
48. **O'Toole, P. W., S. M. Logan, M. Kostrzynska, T. Wadstrom, and T. J. Trust.** 1991. Isolation and biochemical and molecular analyses of a species-specific protein antigen from the gastric pathogen *Helicobacter pylori*. J. Bacteriol. **173:**505–513.
49. **Parkhill, J., B. W. Wren, K. Mungall, J. M. Ketley, C. Churcher, D. Basham, T. Chillingworth, R. M. Davies, T. Feltwell, S. Holroyd, K. Jagels, A. V. Karlyshev, S. Moule, M. J. Pallen, C. W. Penn, M. A. Quail, M. A. Rajandream, K. M. Rutherford, A. H. van Vliet, S. Whitehead, and B. G. Barrell.** 2000. The genome sequence of the food-borne pathogen *Campylobacter jejuni* reveals hypervariable sequences. Nature **403:**665–668.
50. **Pesci, E. C., D. L. Cottle, and C. L. Pickett.** 1994. Genetic, enzymatic, and pathogenic studies of the iron superoxide dismutase of *Campylobacter jejuni*. Infect. Immun. **62:**2687–2694.
51. **Poole, L. B.** 1996. Flavin-dependent alkyl hydroperoxide reductase from *Salmonella typhimurium*. 2. Cystine disulfides involved in catalysis of peroxide reduction. Biochemistry **35:**65–75.
52. **Poole, L. B., H. Z. Chae, B. M. Flores, S. L. Reed, S. G. Rhee, and B. E. Torian.** 1997. Peroxidase activity of a TSA-like antioxidant protein from a pathogenic amoeba. Free Radic. Biol. Med. **23:**955–959.
53. **Poole, L. B., and H. R. Ellis.** 1996. Flavin-dependent alkyl hydroperoxide reductase from *Salmonella typhimurium*. 1. Purification and enzymatic activities of overexpressed AhpF and AhpC proteins. Biochemistry **35:**56–64.
54. **Poole, L. B., A. Godzik, A. Nayeem, and J. D. Schmitt.** 2000. AhpF can be dissected into two functional units: tandem repeats of two thioredoxin-like folds in the N-terminus mediate electron transfer from the thioredoxin reductase-like C-terminus to AhpC. Biochemistry **39:**6602–6615.
55. **Poole, L. B., C. M. Reynolds, Z. A. Wood, P. A. Karplus, H. R. Ellis, and M. Li Calzi.** 2000. AhpF and other NADH:peroxiredoxin oxidoreductases, homologues of low M_r thioredoxin reductase. Eur. J. Biochem. **267:**6126–6133.
56. **Prieto-Alamo, M. J., J. Jurado, R. Gallardo-Madueno, F. Monje-Casas, A. Holmgren, and C. Pueyo.** 2000. Transcriptional regulation of glutaredoxin and thioredoxin pathways and related enzymes in response to oxidative stress. J. Biol. Chem. **275:**13398–13405.
57. **Raudonikiene, A., N. Zakharova, W. W. Su, J. Y. Jeong, L. Bryden, P. S. Hoffman, D. E. Berg, and K. Severinov.** 1999. *Helicobacter pylori* with separate beta- and beta′-subunits of RNA polymerase is viable and can colonize conventional mice. Mol. Microbiol. **32:**131–138.
58. **Riddles, P. W., R. L. Blakeley, and B. Zerner.** 1979. Ellman's reagent: 5,5′-dithiobis(2-nitrobenzoic acid)—a reexamination. Anal. Biochem. **94:**75–81.
59. **Rieder, G., R. A. Hatz, A. P. Moran, A. Walz, M. Stolte, and G. Enders.** 1997. Role of adherence in interleukin-8 induction in *Helicobacter pylori*-associated gastritis. Infect. Immun. **65:**3622–3630.
60. **Salyers, A. A., and D. D. Whitt.** 1994. Bacterial pathogenesis—molecular approach, p. 273–281. ASM Press, Washington, D.C.
61. **Schröder, E., J. A. Littlechild, A. A. Lebedev, N. Errington, A. A. Vagin, and M. N. Isupov.** 2000. Crystal structure of decameric 2-Cys peroxiredoxin from human erythrocytes at 1.7 A resolution. Structure **8:**605–615.
62. **Schröder, E., and C. P. Ponting.** 1998. Evidence that peroxiredoxins are novel members of the thioredoxin fold superfamily. Protein Sci. **7:**2465–2468.
63. **Spiegelhalder, C., B. Gerstenecker, A. Kersten, E. Schiltz, and M. Kist.** 1993. Purification of *Helicobacter pylori* superoxide dismutase and cloning and sequencing of the gene. Infect. Immun. **61:**5315–5325.
64. **Stadtman, T.C.** 1996. Selenocysteine. Annu. Rev. Biochem. **65:**83–100.
65. **Storz, G., F. S. Jacobson, L. A. Tartaglia, R. W. Morgan, L. A. Silveira, and B. N. Ames.** 1989. An alkyl hydroperoxide reductase induced by oxidative stress in *Salmonella typhimurium* and *Escherichia coli*: genetic characterization and cloning of *ahp*. J. Bacteriol. **171:**2049–2055.
66. **Thurman, R. G., H. G. Ley, and R. Scholz.** 1972. Hepatic microsomal ethanol oxidation. Hydrogen peroxide formation and the role of catalase. Eur. J. Biochem. **25:**420–430.
67. **Tomb, J. F., O. White, A. R. Kerlavage, R. A. Clayton, G. G. Sutton, R. D. Fleischmann, K. A. Ketchum, H. P. Klenk, S. Gill, B. A. Dougherty, K.**

Nelson, J. Quackenbush, L. Zhou, E. F. Kirkness, S. Peterson, B. Loftus, D. Richardson, R. Dodson, H. G. Khalak, A. Glodek, K. McKenney, L. M. Fitzgerald, N. Lee, M. D. Adams, J. C. Venter, et al. 1997. The complete genome sequence of the gastric pathogen *Helicobacter pylori*. Nature **388:**539–547.

68. **Ursini, F., M. Maiorino, and C. Gregolin.** 1985. The selenoenzyme phospholipid hydroperoxide glutathione peroxidase. Biochim. Biophys. Acta **839:** 62–70.
69. **van Vliet, A. H., M. L. Baillon, C. W. Penn, and J. M. Ketley.** 1999. *Campylobacter jejuni* contains two *fur* homologs: characterization of iron-responsive regulation of peroxide stress defense genes by the PerR repressor. J Bacteriol. **181:**6371–6376.
70. **Wang, Y., and D. E. Taylor.** 1990. Chloramphenicol resistance in *Campylobacter coli*: nucleotide sequence, expression, and cloning vector construction. Gene **94:**23–28.
71. **Westblom, T. U., S. Phadnis, W. Langenberg, K. Yoneda, E. Madan, and B. R. Midkiff.** 1992. Catalase negative mutants of *Helicobacter pylori*. Eur. J. Clin. Microbiol. Infect. Dis. **11:**522–526.
72. **Wieles, B., D. van Soolingen, A. Holmgren, R. Offringa, T. Ottenhoff, and J. Thole.** 1995. Unique gene organization of thioredoxin and thioredoxin reductase in *Mycobacterium leprae*. Mol. Microbiol. **16:**921–929.
73. **Williams, C. H., Jr., G. Zanetti, L. D. Arscott, and J. K. McAllister.** 1967. Lipoamide dehydrogenase, glutathione reductase, thioredoxin reductase, and thioredoxin. J. Biol. Chem. **242:**5226–5231.
74. **Windle, H. J., A. Fox, D. Ni Eidhin, and D. Kelleher.** 2000. The thioredoxin system of *Helicobacter pylori*. J. Biol. Chem. **275:**5081–5089.
75. **Yamamoto, H., C. Miyake, K. J. Dietz, K. Tomizawa, N. Murata, and A. Yokota.** 1999. Thioredoxin peroxidase in the cyanobacterium *Synechocystis* sp. PCC 6803. FEBS Lett. **447:**269–273.